Sustained *in situ* measurements of dissolved oxygen, methane and water transport processes in the benthic boundary layer at MC118, northern Gulf of Mexico

Christopher S. Martens [a,*], Howard P. Mendlovitz [a], Harvey Seim [a], Laura Lapham [b], Marco D'Emidio [c]

[a] *Department of Marine Sciences, UNC Chapel Hill, Chapel Hill, NC 27599, USA*
[b] *University of Maryland Center for Environmental Science, Chesapeake Biological Laboratory, Solomons, MD 20688, USA*
[c] *Mississippi Mineral Resources Institute, University of Mississippi, University, MS 38677, USA*

ARTICLE INFO

Available online 26 November 2015

Keywords:
Deepwater Horizon
MC118
Dissolved oxygen
Methane
Benthic lander
Internal waves
Benthic boundary layer
Total oxygen utilization
Sediment oxygen demand
Ocean circulation
Continental slope

ABSTRACT

Within months of the BP Macondo Wellhead blowout, elevated methane concentrations within the water column revealed a significant retention of light hydrocarbons in deep waters plus corresponding dissolved oxygen (DO) deficits. However, chemical plume tracking efforts were hindered by a lack of *in situ* monitoring capabilities. Here, we describe results from *in situ* time-series, lander-based investigations of physical and biogeochemical processes controlling dissolved oxygen, and methane at Mississippi Canyon lease block 118 (~18 km from the oil spill) conducted shortly after the blowout through April 2012. Multiple sensor arrays plus open-cylinder flux chambers ("chimneys") deployed from a benthic lander collected oxygen, methane, pressure, and current speed and direction data within one meter of the seafloor. The ROVARD lander system was deployed for an initial 21-day test experiment (9/13/2010–10/04/2010) at 882 m depth before a longer 160-day deployment (10/24/2011–4/01/2012) at 884 m depth. Temporal variability in current directions and velocities and water temperatures revealed strong influences of bathymetrically steered currents and overlying along-shelf flows on local and regional water transport processes. DO concentrations and temperature were inversely correlated as a result of water mass mixing processes. Flux chamber measurements during the 160-day deployment revealed total oxygen utilization (TOU) averaging 11.6 mmol/m^2 day. Chimney DO concentrations measured during the 21-day deployment exhibited quasi-daily variations apparently resulting from an interaction between near inertial waves and the steep topography of an elevated scarp immediately adjacent to the 21-day deployment site that modulated currents at the top of the chimney. Variability in dissolved methane concentrations suggested significant temporal variability in gas release from nearby hydrocarbon seeps and/or delivery by local water transport processes. Free-vehicle (lander) monitoring over time scales of months to years utilizing *in situ* sensors can provide an understanding of processes controlling water transport, respiration and the fate and impacts of accidental and natural gas and oil releases.

1. Introduction

Monitoring temporal variability in bottom water oxygenation, sediment oxygen demand and physical parameters within the deep-sea benthic boundary layer (BBL) can provide critical information about biogeochemical processes controlling carbon cycling near the seafloor. Time-series data within the BBL is thus essential in efforts to quantify the impacts of major disturbance events affecting the benthic environment. Recent examples of such accidental disturbance events include the deposition and accumulation of hydrocarbon-enriched sediments (Chanton et al., 2012; Joye et al., 2014; Passow, 2016) resulting from the accidental BP Macondo Wellhead oil and gas Blowout (MWB) and Deepwater Horizon disaster. A better understanding of the impacts on benthic environments of both accidental and natural hydrocarbon releases requires *in situ* monitoring of key parameters over time periods that allow for quantification of the rates and mechanisms of controlling processes and a capability to distinguish between sources. In upper slope environments of the northern Gulf of Mexico, major

* Corresponding author. Tel.: +1 919 962 0152.
E-mail addresses: cmartens@email.unc.edu (C.S. Martens), mendlovitz@unc.edu (H.P. Mendlovitz), hseim@email.unc.edu (H. Seim), lapham@umces.edu (L. Lapham).

http://dx.doi.org/10.1016/j.dsr2.2015.11.012

disturbance events include accidental petroleum releases such as the MWB (Joye et al., 2011), tectonic activity that results in releases of hydrocarbons from natural gas and oil seeps (Lapham et al., 2013; MacDonald et al., 2000; Macelloni et al., 2012; Mau et al., 2007), seasonal storm events that can enhance mixing (A. Bracco, personal communication) and the formation and dissolution of gas hydrates (Lapham et al., 2014; MacDonald et al., 1994). The rapid response to the MWB has led to continuing investigations such as the ECOGIG (Ecosystem Impacts of Oil and Gas Inputs to the Gulf) project funded by the Gulf of Mexico Research Initiative (GoMRI) that have allowed for multi-investigator, coordinated efforts to quantify both short- and long-term ecosystem responses in both the water column and the sediments regardless of whether the hydrocarbon releases are natural or anthropogenic. However, simultaneous time-series measurements of biogeochemical processes and bottom water transport in BBL of the dynamic and hydrocarbon-rich upper slope environments of the northern Gulf have rarely been made at the needed temporal scales.

Here we present results from a time series study of the biogeochemical and physical transport processes that control dissolved oxygen (DO) and methane concentration distributions within the BBL and sediment oxygen utilization at two upper slope sites in the northern Gulf of Mexico near the MWB. For the purposes of this study we define the BBL as the water column within one meter of the seafloor, approximating the definition of the logarithmic layer described by Dade et al. (2001). The two sites, located within 20 km of the MWB, featured active nearby natural gas and oil seeps as well as shallow gas hydrate occurrences. The primary objectives of the lander experiments were to determine the processes controlling temporal variability in dissolved oxygen and methane concentrations plus water transport processes occurring within a meter of the seafloor in this area of the northern Gulf which is known for occurrences of natural oil and gas seep sites and the presence of gas hydrates (Lapham et al., 2008b; Macelloni et al., 2012; McGee, 2006; Sassen et al., 2006). Sustained *in situ* measurements of these processes are needed to quantify both immediate impacts of oil and gas release and to understand the long-term responses by the benthos associated with hydrocarbon degradation. Sustained time series measurements are also of great interest for understanding the processes controlling the occurrence and stability of gas hydrates (e.g. Lapham et al., 2013', 2008a; Macelloni et al., 2013; Torres et al., 2007) and the resilience of the highly diverse, coldwater coral ecosystems (Davies et al., 2010; Mienis et al., 2012; White et al., 2012) found in continental slope environments throughout the world ocean (Roberts et al., 2009).

The experimental work was accomplished using two deployments of autonomous benthic landers at 882 and 884 m depth, respectively, at Mississippi Canyon lease block 118 (MC118) in 2010 and 2011–2012. The landers were equipped with advanced *in situ* sensor arrays to continuously monitor ambient DO, temperature and physical parameters including pressure (depth) and current speed and direction at approximately one meter above the seafloor for sustained periods. In addition, we utilized a simple new approach to continuously measure sediment total oxygen utilization (TOU; as defined by Glüd (2008) based on an open cylinder flux chamber system called the Chimney Sampler Array (CSA). The open chimney design avoids complete DO reduction in sealed chambers or the induction of methane hydrate formation during light hydrocarbon gas bubble release known to occur at gas-rich northern Gulf sites. Our “open chimney” approach to measuring TOU adds to a range of previously developed methods that include fluxes calculated from porewater DO concentration gradients measurements using microsensors (Røy et al., 2005; McGinnis et al., 2014), closed chamber time-series measurements (Glüd et al., 1995; McGinnis et al., 2014), eddy correlation techniques (McGinnis et al, 2014) and combined measurements of DO and nutrient vertical concentration gradients in the BBL to calculate relative DO fluxes (Glüd et al., 2007; Holtappels et al., 2011).

1.1. Study site

Mississippi Canyon Lease Block 118 (MC118) described by Macelloni et al., (2013; 2012) includes an area on the Gulf of Mexico seafloor (Fig. 1) with several natural seep features collectively known as Woolsey Mound. Woolsey Mound has previously been chosen as a gas hydrate observatory site (McGee, 2006) named in honor of the late Robert Woolsey. Within MC118, there are three distinct crater provinces showing different seafloor features. The northwest (NW) crater complex includes gassy muds, microbial mats, oily sediments, chemosynthetic communities and deep sea corals; the southwest (SW) crater complex includes an active hydrocarbon seep area and includes large outcrops of gas hydrate, microbial mats, carbonate blocks, chemosynthetic communities and deep sea corals; the southeast (SE) crater complex shows little evidence for active gas seepage at present but contains numerous dead clam shells potentially associated with previous hydrocarbon availability. Microbial mats are prevalent throughout the entire MC118 area and generally represent sites where methane reaches shallow sediment depths (Lloyd et al., 2010). The variability in seafloor expressions and evidence for microbial activity led Lapham et al. (2008b) to hypothesize that these different crater areas represented a temporal series of seafloor environments produced by changes in seepage rates occurring on time scales of at least years. Hydrocarbon seepage at the SW crater is thought to have been ongoing for years or longer while the NW crater region is hypothesized to represent a relatively new vent regime. However, visible seepage at the SE area appears to have ceased. All three crater areas are directly associated with different master faults tied to the deep hydrocarbon reservoir (Macelloni et al., 2012; Simonetti et al., 2013). Recently, a pockmark feature was found along the eastern most fault in MC118 suggesting active gas venting (Simonetti et al., 2013), however, elevated methane concentrations were not found during water column profiling (Wilson et al., 2014). A recent chemostratigraphy study based on analysis of shallow gravity core data in the Woolsey Mound area revealed that terrigenous sediment burial is the primary control on temporal changes in sediment composition and suggested a relatively stable sedimentation pattern during the late Pleistocene and Holocene (Ingram et al., 2013). However, Ingram et al. (2013) found evidence for more dynamic depositional patterns immediately adjacent to the salt diapirism-induced bathymetric high. The variable environmental conditions found within MC118 make it an ideal place to study temporal variability in biogeochemical processes associated with oil and gas seepage including temporal variability in dissolved oxygen and methane concentrations within the BBL.

2. Materials and methods

2.1. ROVARD lander

The ROVARD lander used in our experiments was developed at the Center for Marine Resources and Environmental Technology at the University of Mississippi. The ROVARD lander is built around the basic concept of a pop-up buoy where a weighted platform is set on the seafloor using a trawl cable and acoustic releases (Sleeper et al., 2011). The lander mainframe used in our experiments included a recovery line storage drum, clutch system, two 866 Benthos acoustic releases, ten 17” Benthos spheres and two 40 AH DeepSea Power and Light batteries. Positioning of the lander

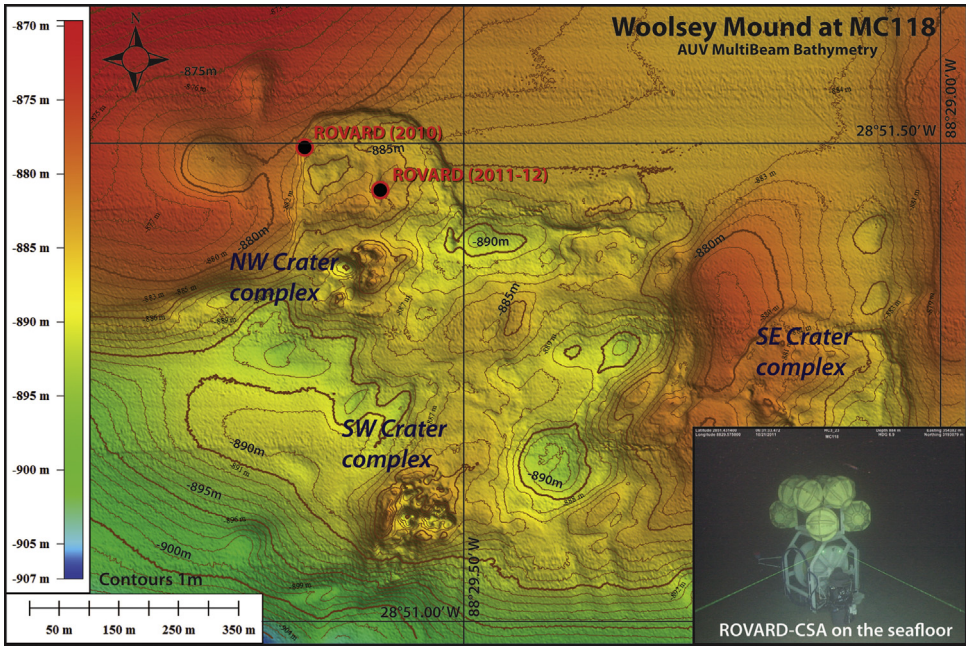

Fig. 1. Bathymetric map showing sites of ROVARD lander deployments within lease block MC118. Photo courtesy Erik Cordes, NRDA project/E/V *Nautilus* and ROV *Hercules* ©2011.

on the seafloor was aided by Ultra Short Base Line (USBL) acoustic transponders. To recover the platform, the series of floats tethered to the reel of lifting line was acoustically released and hauled aboard with the ship's A-frame and winch.

2.2. The Chimney Sampler Array (CSA)

Custom mounts were fabricated to place our multi-sensor systems in optimum positions for measurements at less obstructed positions on the ROVARD platform itself or to allow for ROV-assisted seafloor deployments of cabled sensors at distances of several meters away from the lander. The Chimney Sampler Array (CSA) consists of one or two independent, open PVC chimney cylinders equipped with sensors attached to data communications and power through 15 m data and strength member cables connected to data loggers located on the ROVARD mainframe. Each 90 cm tall, 30 cm ID chimney is fully open at the top and bottom and has a flared "skirt" consisting of a nylon mesh pouch containing lead pellets attached outside the bottom edge of the cylinder-the weighted skirt helps to create a seal against the sediment surface at the chimney edge without significantly disturbing the sediment surface inside the chimney cyclinder. One or two chimneys were placed on the lander platform. Chimneys are deployed and sealed against the sediment surface either by spring-loaded arms on the ROVARD lander that force their bottom, skirted edges against the surface immediately adjacent to the lander or by a ROV that pulls the chimneys off the lander and places them up to 10 m away. The chimney design provides a simple way to slow turbulent mixing next to the sediment–water interface through trapping ambient water in the open cylinder chimney sealed against the seafloor. The open-top cylinder design prevents hydrate formation known to occur at upper slope pressures and temperatures in the presence of saturation gas concentrations that could occur during gas bubble release, a frequent occurrence in gas-rich northern Gulf sediments (e.g. MacDonald et al., 1994).

Dissolved O_2 (DO) measurements inside chimneys were utilized to provide quantitative information about the relative magnitude and temporal variability in TOU. TOU includes both oxygen utilization by the benthos and diffusive oxygen uptake (DOU) so it is consistently greater than DOU (Glüd, 2008) and includes the effects of macrofaunal respiration and sediment topography (Røy et al., 2005). The dominant processes controlling internal chimney water DO concentrations are expected to be washout (water renewal) rates through the open chimney top and TOU. The former should be a function of current velocity and resulting turbulent mixing (e.g. McGinnis et al., 2014), thus a gradient in O_2 concentrations within the chimney, particularly near the sediment surface, should be greater during periods of low current velocity and should provide a quantitative measure of TOU if eddy diffusivities within the chimney were known. Differences between ambient DO concentrations outside the chimney and within the chimney could also provide a qualitative measure of the relative importance of TOU influence. We assumed that the 30 cm ID of the chimney would restrict the scale of turbulent eddies and placed optode DO sensors at 20.3 and 28.4 cm heights above the bottom inside the chimney in order to assess the magnitude of resulting concentration gradients within the chimney. We also measured ambient DO in the BBL at approximately 1 m off the bottom continuously throughout the experiments.

2.3. Sensor instrumentation

During our longer 160-day deployment in 2011–2012, an AADI (Aanderaa Data Instruments) Seaguard logger unit rated to 6000 m collected data from three oxygen optodes (AADI model 4330) that also provided temperature data, one pressure (depth) sensor (model 4117), one conductivity (model 4319) and one current sensor (Z-Pulse, single point, model 4520 acoustic Doppler) located 1 m above the seafloor. This sensor array was duty cycled every 2 min in order to obtain measurements for a projected monitoring period of six months using two internal Li batteries with total power availability of 70 Ah at 7 V. One of the O_2 optodes was mounted on the ROVARD mainframe approximately 46 cm above the seafloor in order to obtain ambient concentration data. As stated above the other two O_2 optode sensors were mounted at 20.3 and 28.4 cm respectively above the seafloor inside a single chimney.

During a shorter 21-day test deployment in 2010, a METS methane sensor (Franatech GmbH) was deployed and independently cabled to a second Seaguard logger unit (0–6000 m). The METS was mounted

on the exterior of the chimney in order to determine ambient water concentration values. We chose to isolate power to the METS sensor from a pair of SeaBatteries (DeepSea Power and Light) with approximately 80 AH total capacity at 24 V because of the relatively high power demand resulting from sensor warm-up. The METS sensor measured methane data in two modes: It was turned on and continuously collected data for 5 min every 2 h during the full 21 day deployment; every other day it was also turned on for a continuous four hour period to allow complete warm-up plus several hours of data collection. The available power was projected to allow methane measurements for a period of several weeks. We did not include the METS sensor on the longer lander deployment because of power limitations.

2.4. Sensor measurement precisions

Oxygen optodes were re-calibrated in batches of seven in our laboratory. An average precision of ≤ 2 μM was obtained for the optodes used in our deployments at MC118. Analytical precision for optode temperature measurements was ± 0.0001 °C. Conductivity was measured at an accuracy of ± 0.0018 S/m PSU. Accuracies for AADI Z-Pulse current velocity and direction measurements were ± 0.15 cm/s and $\pm 5°$ respectively. The specified range for the METS sensor measurements was 50 nM–10 μM.

2.5. ROVARD lander deployments

CSA time-series measurements were made at two sites within MC118 (Fig. 1) located approximately 18.371 and 18.211 km to the northwest of the Macondo Wellhead blow-out that occurred in Mississippi Canyon lease block 252 (MC252). The first series was a short test deployment during which data was collected for 21 days from 13 September to 4 October 2010 before ROVARD recovery on 28 June 2011. For this initial 21-day test experiment we used a ROV operated from the RV *Pelican* to deploy a CSA system with a single chimney at Woolsey Mound at an average depth of 882 m at a station located in close proximity (Latitude 28° 51.47400' N, Longitude 88° 29.65702' W; see Fig. 1) to an easily recognizable "horseshoe" shaped scarp associated with salt dome tectonic activity (Macelloni et al., 2013). During this test lander experiment, but after *in situ* measurements had ceased due to power limitations, a BOEM/NOAA project *Lophelia* II cruise led by Chief Scientist, Chuck Fisher, visited the ROVARD deployment site on November 18, 2010 and utilized the Jason II ROV (WHOI) to find and photograph the lander on the seafloor, verifying that the chimney was well-situated on the sediment surface.

The ROVARD with the CSA system on board was deployed a second time for 160 days from 24 October 2011 to 1 April 2012, and deployed one chimney using its spring-loaded arms without a ROV. The site chosen for this longer data collection period was to the south of the "horseshoe" shaped scarp associated with salt dome tectonic activity (Macelloni et al., 2013) within the NW province (Latitude 28°51.42232' N, longitude 88°29.57791' W, Figs. 1 and 2). The ROVARD was deployed on October 15, 2011, at an average depth of 884 m and sensor measurements began on October 24, 2011. The ROV *Hercules*, deployed from the E/V *Nautilus* during a NDRA cruise led by Chief Scientist Eric Cordes, took the photo insert of the ROVARD seen in Fig. 1. The site, a slight seafloor depression in seafloor topography which we will refer to as the "crater" (Fig. 2), featured a high density of *pogonophora sp* occurrences plus microbial

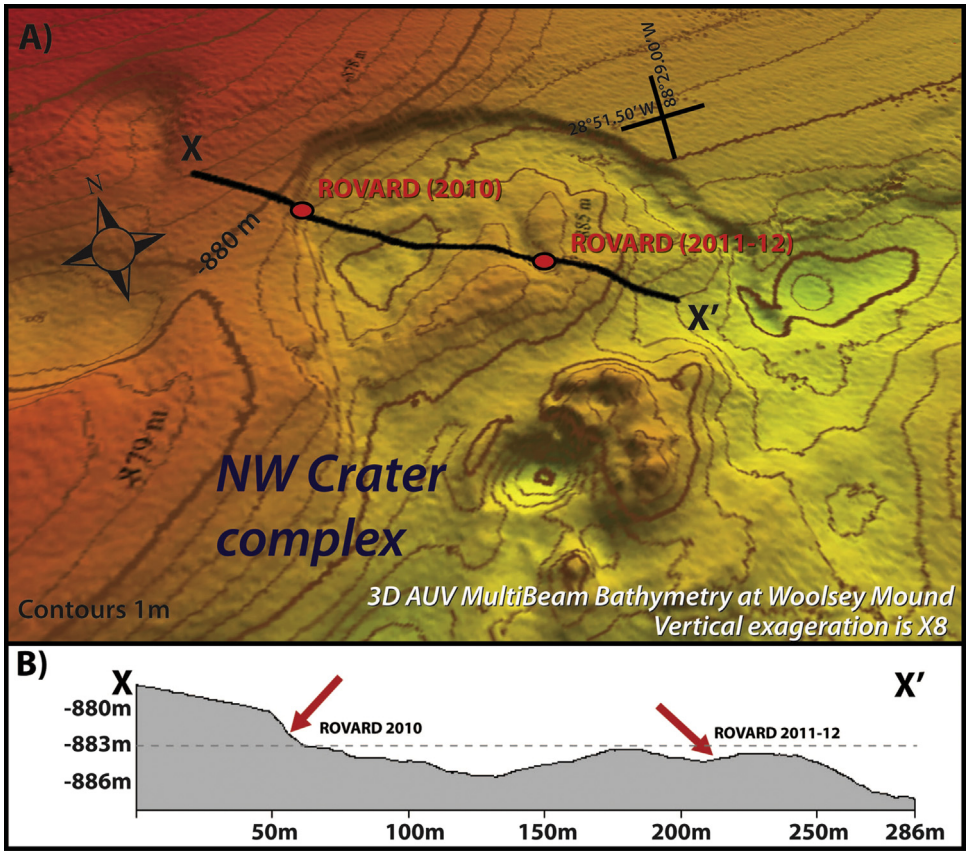

Fig. 2. (A) 3D image of the Woolsey Mound NW Crater Complex showing the morphology of the two ROVARD-CSA deployment sites. (A) Contours = 1 m. (B) Bathymetric profile across the deployment sites indicated by red arrows. (For interpretation of the references to color in this figure legend, the reader is referred to the web version of this article.)

mats and abundant live clam shells generally associated with methane seepage (Lapham et al., 2008b; Lloyd et al., 2010; Macelloni et al., 2013). The fine-grained sediments at the site were abundantly pitted and released bubbles when disturbed. The ROVARD lander was successfully released from the seafloor by an acoustic release triggered by the surface ship RV *Pelican* and recovered on April 1, 2012, with all sensors intact.

3. Results

3.1. Time series CSA results from the 21-day test deployment at MC118

Results of continuous CSA sensor measurements from the 21-day test deployment are illustrated in Fig. 3. The water depth for the pressure (depth) sensor mounted on the lander 0.5 m above the seafloor ranged from 881.5 to 883.1 m (Fig. 3d). Slight systematic downward drifts in pressure values suggested possible sensor calibration issues or slight downslope sliding movement of the lander. The November 2010 ROV visit showing the chimney still located about 5 m away supports the former explanation. Ambient DO concentration values averaged 141.1 ± 2.0 μM (Fig. 3a) and temperature data from all three optodes was in close agreement (Fig. 3b). DO concentrations within the chimney were always lower than ambient as expected and exhibited interesting, quasi-periodic minima at roughly daily intervals (Fig. 3a). The methane concentrations measured by the METS sensor (Fig. 3c) should be viewed as approximate values because the sensor membrane was not capped with a pumped flowcell because of power limitations and thus would have reacted slowly to changes in ambient methane. However, the observed values up to almost 2 μM are within the 3 nM to over 2 μM range previously observed in the BBL at lease block MC118 from a Pore Fluid Array sampler collecting overlying water samples over a four month period (Lapham et al., 2008a, 2008b) and by underwater Membrane Introduction Mass Spectrometry (MIMS) in June 2010 (T. Short, personal communication, 2013).

3.2. Time series results from the 160-day deployment at MC118

Data obtained by CSA sensors during the 160 day deployment are illustrated in Figs. 4 and 5 and described in more detail below. We time-averaged the data collected every 2 min for one hour because no significant signals were present at frequencies greater than a cycle per hour and because of intermittent high-frequency noise on some of the channels that did not affect averaged data.

3.2.1. Temperature, salinity and DO

Temperature ranged from 4.6 to 6 °C (Fig. 4b) and exhibited weekly to monthly period fluctuations up to 0.5 °C. Temperature was above 5 °C except for a week-long period in late November, 2011. The mean value was 5.42 °C. Salinity was relatively constant at 34.9 ± 0.1 PSU (data not shown). Temporal variability in ambient DO exhibits a substantial range of 135–175 μM (Fig. 4a) that correlates negatively with temperature changes. This correlation also holds for a secondary peak in temperature variability at inertial periods (roughly 24 h). The mean ambient DO value was 147.7 μM. DO concentrations within the open cylinder chimneys ranged from near ambient values to near zero concentrations at 20.3 cm and 28.4 cm above the sediment surface. These data are shown and discussed in Section 4.3.

3.2.2. Tidally controlled pressure (depth) variation

Water depths (Fig. 4c) from the pressure sensor attached to the lander at 50 cm above the seafloor at the crater site ranged from 882.3 to 883.1 m; mean = 882.67 m, with variability dominated by the tides. Tidal analysis indicates that more than 90% of the variance is due to the strongly diurnal tide, dominated by O1 and K1, both with amplitudes of approximately 14 cm, consistent with existing tidal charts for the north Gulf of Mexico (Seim et al., 1987). A clear fortnightly signal modulated the water level (WL) variations. Maximum variation was about one meter.

3.2.3. Current velocities and directions

Current velocity and direction data are plotted in Fig. 5a and b. The average speed for the entire 160-day measurement period was 6 cm/s. The range of hourly velocities observed was 0.1–22.3 cm/s.

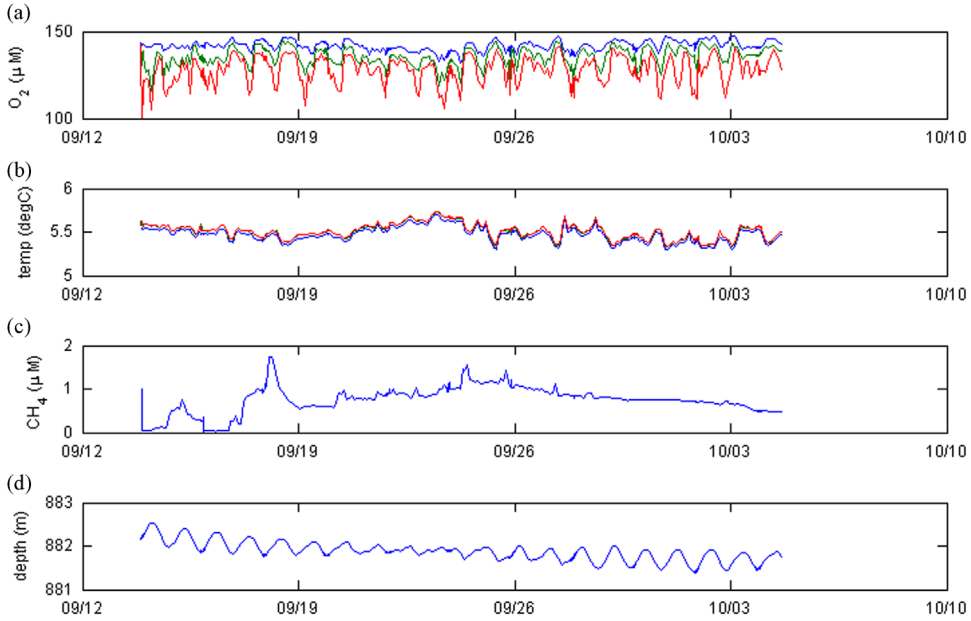

Fig. 3. 21 day test deployment observations of (a) ambient DO concentrations (blue), internal chimney DO concentrations: green (25.4 cm above seafloor) and red (20.3 cm above seafloor), (b) ambient (blue) and internal chimney (red) temperatures, (c) ambient methane concentration, and (d) depth. (For interpretation of the references to color in this figure legend, the reader is referred to the web version of this article.)

Several bursts of velocities greater than 9 cm/s occur over the measurement period, each lasting for 2–7 days.

4. Discussion

4.1. Chimney DO variability during 21-day deployment

DO concentrations within the chimney exhibited an irregular but approximately daily variation of 5–25 μM (Fig. 3a). Though similar in period to the regular water level variations, a careful comparison indicates that the variations are not coherent, with the timing of maxima of the two signals changing over the deployment period; thus the DO variability is not tidal. Temperature variations, though small (< 0.4 °C), are coherent with the DO variations, with cooler temperatures associated with higher DO concentrations. We hypothesize that these near daily variations in DO and temperature are produced in response to internal wave forcing at near inertial frequencies, which at this latitude is 24.8 h. Near inertial waves will produce flow of nearly equal strength but

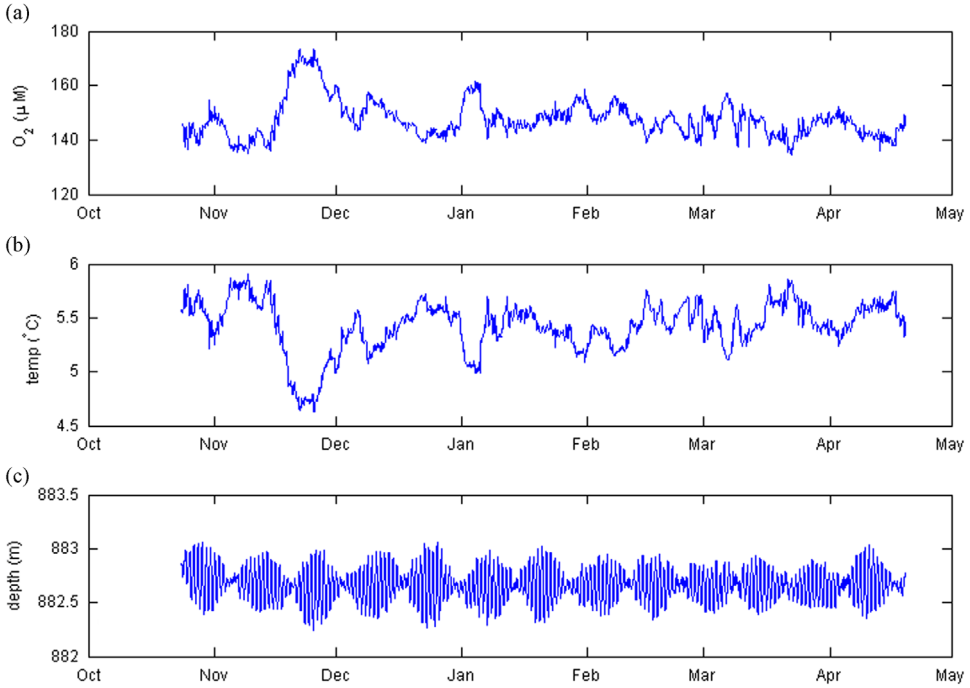

Fig. 4. 160 day deployment results from the CSA. Hourly averages of ambient (a) DO concentrations and (b) temperature and (c) depth.

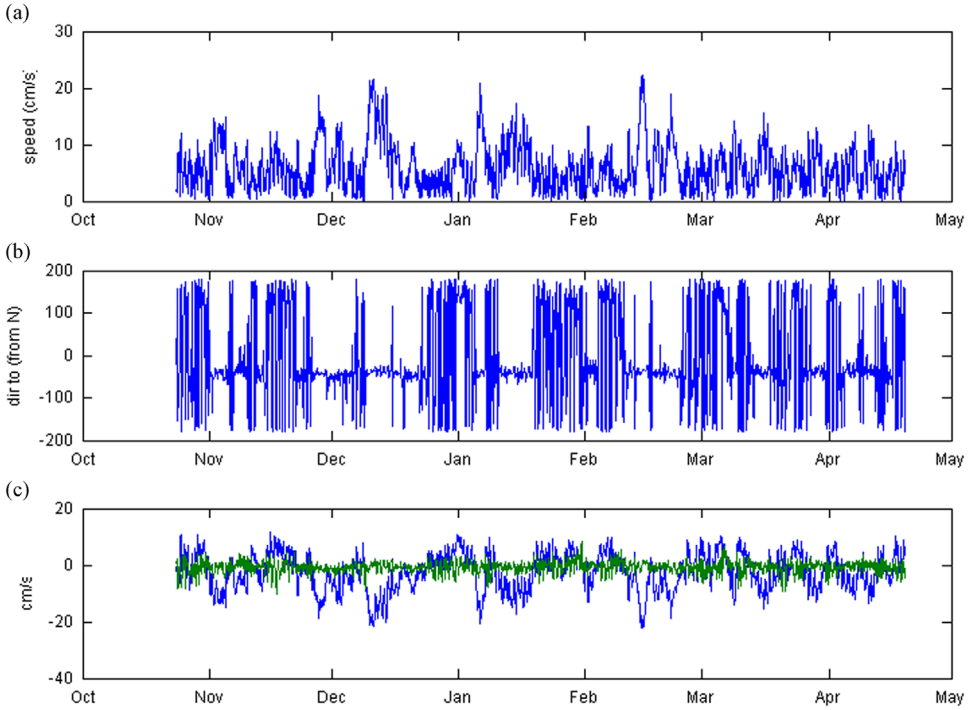

Fig. 5. Time series of hourly values of (a) current speed, (b) current direction, and (c) cross-slope current speed (blue, positive downslope, towards 142°) and along-slope current speed (green). (For interpretation of the references to color in this figure legend, the reader is referred to the web version of this article.)

that rotates in direction over the inertial period. One likely scenario is that flow during one phase of the wave is blocked by the wall of the "horseshoe" scarp (Fig. 2), producing reduced velocities and lower DO concentrations in the chimney due to TOU, while at other times the flow is stronger when not blocked by the nearby topography and more effectively flushes the water in the chimney, leading to higher DO concentrations.

4.2. In situ methane time-series measurements during 21-day deployment

Our 16 days of continuous methane time series measurements from the test deployment (Fig. 3) are among the first such data collected from free vehicles in the deep sea due to previous sensor designs and power limitations. Offshore Vancouver Island, a 10 day methane time-series collected near outcropping gas hydrate found methane increases to correlate with shifting bottom currents (Thomsen et al., 2012). However, no such sensors were deployed during the Deepwater Horizon disaster due to sensor design limitations at the time. Therefore, we sought to attain the longest possible record with a new type of METS sensor designed specifically for cold, deep water use and that utilized less power than previous models. The METS sensor was calibrated in collaboration with engineers at Franatech GmbH. We had insufficient lander battery power with which to employ a continuously pumped, flow-through cell over the sensor membrane. Such pumping would have allowed for faster and more accurate measurements of in situ values. However, the methane-rich nature of sediments in the NW crater suggested that we might be able to document concentration values in excess of atmospheric equilibrium values expected to be less than 3 nM Observed concentrations generally exceeded 1 μM with spikes up to nearly 2 μM, likely reflecting methane sediment water inputs via gas bubble releases and possibly the dissolution of exposed methane hydrates common to the NW crater area. These values were similar to what was found previously (Lapham et al., 2008a, 2008b).

4.3. Upslope flow at the MC118 crater site during 160-day deployment

Recent lander measurements on the seafloor at nearby Viosca Knolls (VK826) elucidate the nature of near-bottom water transport processes in upper slope environments of the northern Gulf of Mexico (Davies et al., 2010; Mienis et al., 2012). At a depth of approximately 500 m the overlying flow 50–150 m above bottom strongly influenced transport within 50 m of the seafloor and was dominated by weekly to monthly current fluctuations in the along-slope direction that reached peak speeds of 60 cm/s at 50–100 m above the seafloor. This vertical structure is consistent with slope-trapped waves found to dominate the flow regime of the upper slope in the northern Gulf between DeSoto and Mississippi Canyons in a large multi-year observational study (Carnes et al., 2008; Hallock et al., 2009). At VK826 the flow in the lowest 50 m above the bottom slowed and veered counter-clockwise closer to the seafloor, consistent with a bottom Ekman layer, producing a cross-slope component to the flow that increased in strength towards the bottom. Bottom temperature variations were strongly correlated to along-slope flow 50–100 m above the seafloor, with westward flow producing warming and eastward flow cooling as a result of cross-slope transport of the mean vertical structure. Bottom topography was seen to impact flow direction in the lowest few meters above the seafloor, as one of two landers deployed by Davies et al. (2010) near steep bottom topography measured flow directions quite different from the overlying flow (Mienis et al., 2012).

Observations at MC118 find NW (upslope) flow to produce warming during our 160-day lander deployment. This result is surprising because NW flow over smooth topography in the northern Gulf would be expected to deliver cooler water. The rough topography surrounding the lander (Fig. 2) may provide an explanation. The larger scale overlying flow is expected to follow the larger scale topography and thus to follow isobaths in the ENE-WSW direction. WSW overlying flow would be expected to drive downslope flow in the bottom boundary layer and be associated with warming temperatures. The crater in which the lander was deployed may fill in such a way that the center of the crater, at the position of the lander, experiences NW flow when the overlying flow is WSW, filling the crater with warmer water. Overlying flow to the ENE may produce the opposite effect, bringing cooler water upslope but which fills the center of the crater with flow towards the SE.

4.4. Bathymetric controls on local currents within the BBL

Current speeds ranged from near zero to over 22 cm/s in bursts sustained for multiple days (Fig. 5). The mean (vector-averaged) current over the deployment period was 2.6 cm/s toward 305°. Decomposing the flow along the principal axis (307°, defined by the variance ellipse) reveals that the currents were largely rectilinear, predominantly SE to NW, with NW flow confined to a narrow range of directions (Fig. 5c). The directionality is consistent with and parallel to the local topography (see Figs. 1 and 2). The strongest currents were towards 320°; nearly all flow greater than 15 cm/s was in this direction.

To examine the relationship between the currents and temperature we performed a cospectral analysis of the cross-slope component of the current and the temperature. The analysis can be used to identify the frequencies at which the two variables covary and to confirm if the oscillations are coherent, and if so, the phase relationship between them. Two distinct bands of energy are present in the cross amplitude spectrum (Fig. 6a) of the current in the upslope direction and temperature: at low frequencies (weekly to monthly) and at inertial frequencies (~24 h). The cospectral analysis indicates these two variables are significantly coherent in both frequency bands and that NW flow leads temperature increases by roughly 90° where the two signals are coherent (Fig. 6b and c). These findings suggest that temperature variability at the site is driven largely by cross-slope flow in the boundary layer advecting the cross-slope temperature gradient.

4.5. Temporal variability in ambient dissolved oxygen in the BBL

Our recent measurements of DO concentrations in the deep water column near MC118 in the northern Gulf of Mexico have revealed values typically increasing from less than 120 μM at 500 m depth to over 160 μM at 1000 m depth (King et al., 2015). At depths near 882 m, temporal DO concentrations should largely reflect the dominant influence of Antarctic Intermediate Water (AAIW) (Jochens and DiMarco, 2008; Sturges and Lugo-Fernandez, 2005; Rivas et al., 2005) brought in by the Loop Current (LC) with temporal variations controlled by mixing with Tropical Atlantic Central Water (TACW; Morrison et al., 1983). AAIW features temperatures ranging from 4 to 7 °C.

A nearly linear inverse relationship with temperature (Fig. 7; $[DO] = 306.8 - 29.3T$, $R^2 = 0.98$), consistent with cross-slope advection of vertically-variable water masses explains the bulk of variability observed in our ambient DO levels (Fig. 4). These results indicate changes in ambient DO are largely driven by cross-slope transport in the BBL.

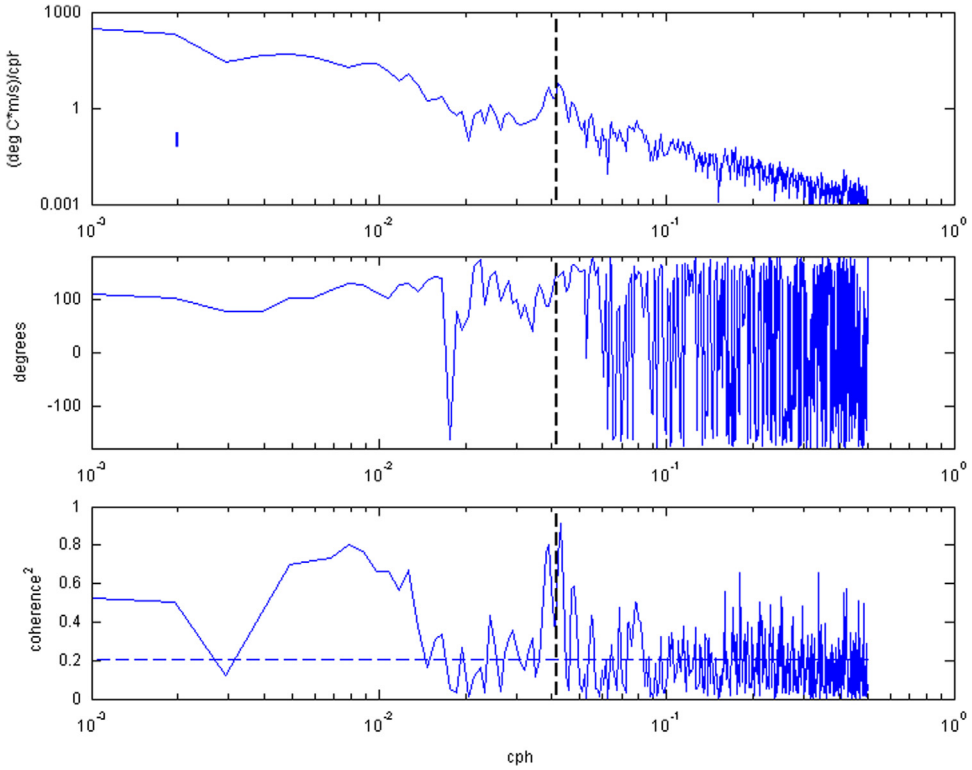

Fig. 6. (a) Cross-amplitude spectrum, (b) phase spectrum, and (c) coherence spectrum as a function of frequency in cycles per hour (cph) of flow along the principal axis and temperature. The vertical dashed line in each plot marks the daily frequency. 95% confidence levels are denoted by the small vertical line in (a) and by the dashed line in (c).

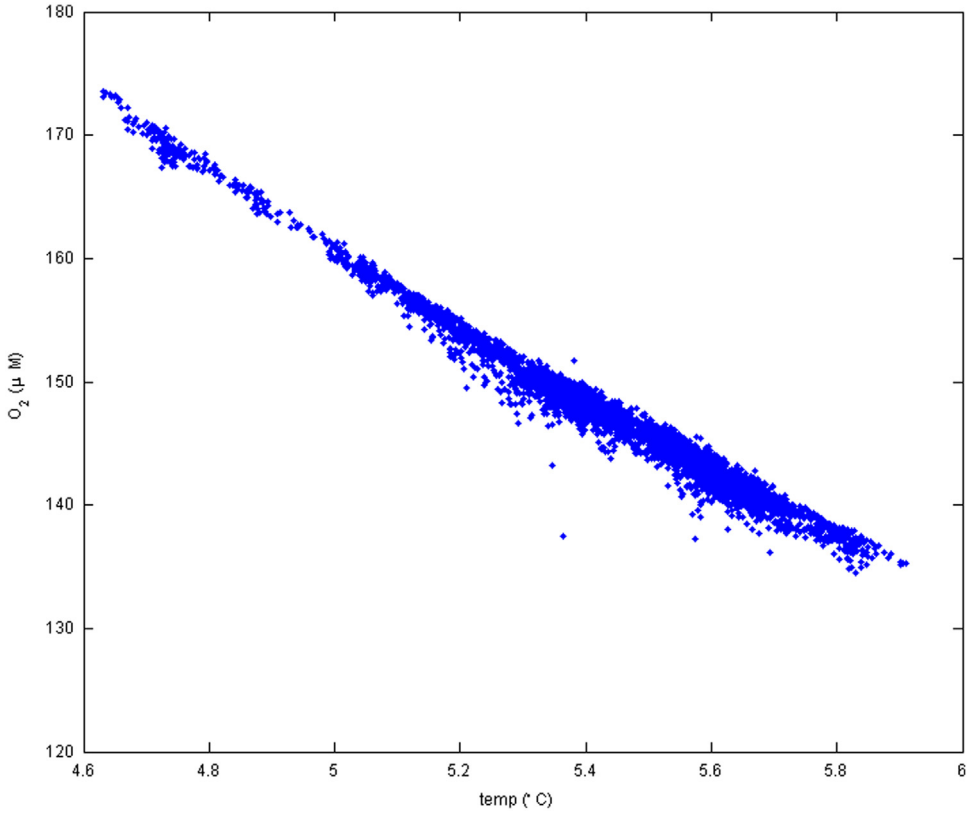

Fig. 7. Scatter plot of ambient DO concentration versus water temperature.

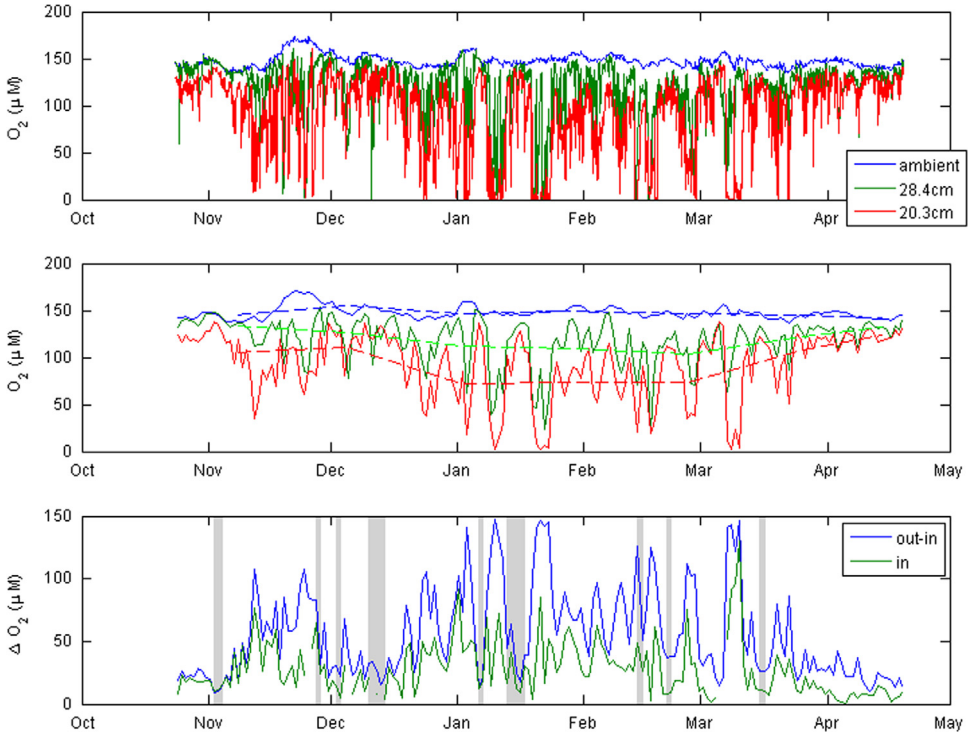

Fig. 8. 160 day deployment: (top panel) ambient hourly DO (blue), internal chimney DO concentrations at 28.4 cm (green) and 20.3 cm (red) above the sediment surface; (middle panel) daily (solid) and 4-week (dashed) averaged values; (bottom panel) DO difference between ambient and 20.3 cm inside chimney (blue) and between the two internal sensors (green). Vertical shading shows times when the daily-averaged current speed was greater than 9 cm/s. (For interpretation of the references to color in this figure legend, the reader is referred to the web version of this article.)

4.6. Turbulent washout versus sediment TOU controls on chimney DO concentrations

DO concentrations within the open cylinder chimney exhibited extreme variability that should be controlled by chimney water washout by turbulent mixing with ambient water combined with DO consumption by sediment TOU. Hourly concentrations measured within the chimney ranged from near ambient values (blue line) to near zero concentration values measured by optodes located at 28.4 cm (green line) and 20.3 cm (red line) above the sediment surface (Fig. 8a). The relative importance of sediment TOU is illustrated by the consistent differences between these two optode data sets, shown for daily and 4-week averaged values in Fig. 8b. The concentration difference within the chimney averages 28 μM over the 160 day period.

The difference between daily-averaged ambient DO and at the lower chimney sensor (blue line) and the difference between the chimney sensors (green line) are plotted in Fig. 8c. The gray shaded regions are time periods when there are strong upslope flows (daily averaged current greater than 9 cm/s). It is clear that strong current events limit the magnitude of the DO deficit, both within the chimney and relative to ambient waters. However, plotting horizontal current speeds versus the DO concentrations within the chimney at both heights above bottom reveals no simple correlation between those parameters (data not shown). The variability in the DO drawdown within the chimney suggests that TOU may have varied over the time of the deployment. In a study of benthic DO exchange in permeable, sandy sediments on the Baltic shelf, McGinnis et al. (2014) compared results from eddy correlation, closed benthic chamber and sediment DO microprofiling techniques. They concluded that observed high variability in exchange rates resulted from a combination of changes in benthic hydrodynamics, sediment permeability and sediment redox conditions. We considered using one of these techniques before devising a simple approach using our chimneys and current speed data. There is far less DO penetration in the muddy sediments at our upper slope sites in the northern Gulf which would make microprofile measurements difficult to achieve. Closed benthic chamber methods that included automated opening and closing (and other capabilities beyond our current capabilities) were not possible. The eddy correlation method should be an applicable approach at our sites, however, problems with the utility of fragile, fast-response, Clark-type needle sensors and deep-sea deployments of ADV systems precluded their use in our longer term, time-series studies using relatively simple lander gear. We thus sought to exploit our observations of a systematic relationship between variable current speeds and optode DO gradient measurements to provide at least maximum estimates of sediment TOU. Before deploying the chimneys in the lander field experiments, we utilized fluorescein dye and particle imaging velicometry to perform rudimentary, qualitative tests to examine turbulent mixing in scaled-down, open cylinder models in a large flume facility in the Fluids Laboratory at UNC-Chapel Hill. We observed active turbulent mixing throughout the cylinder at horizontal current speeds ranging from 5 to over 20 cm/s.

We can estimate sediment TOU as the product of an eddy diffusivity K and the gradient of DO between the pair of optode sensors at two different heights within the chimney:

$$F = K(\Delta \mathrm{DO}/\Delta z) \tag{1}$$

We estimate $K = \kappa z u_*$, assuming turbulent boundary layer dynamics (Trowbridge et al., 1999), where κ is von Karman's constant ($=0.4$), z is height above the bed, and u_* is the friction velocity. The friction velocity is estimated using a quadratic drag law with a drag coefficient $C_d = 1 \times 10^{-3}$, and assumed to be a constant over the height of the chimney. We replace the length

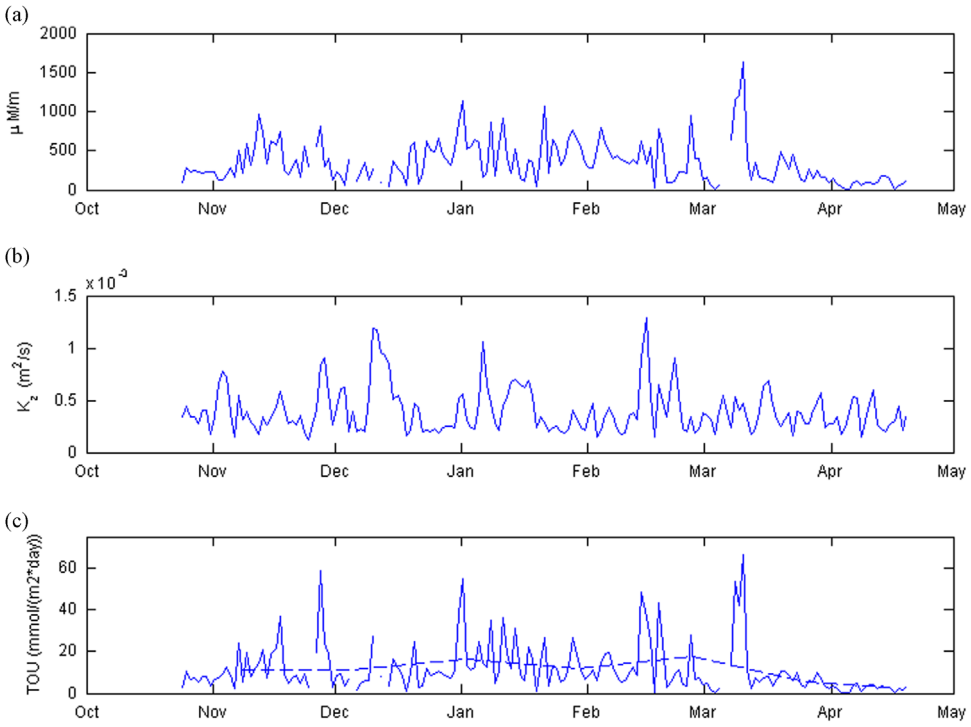

Fig. 9. Daily-averaged (a) observed DO concentration gradient, (b) estimated maximum eddy diffusivity in the chimney, and (c) potential TOU. Four week averaged TOU is shown in (c) as a dashed line.

scale z with the diameter of the chimney (0.3 m) to represent the maximum scale of turbulent eddies. This estimate of the eddy diffusivity should be considered a maximum value, assuming some decay of turbulence within the chimney away from its opening at the top. For the same reason our calculated TOU values should be regarded as maximums. Calculated concentration gradients, eddy diffusivities and TOU shown in Fig. 9 have deployment-long means of 351 μM/m, 3.96×10^{-4} m^2/s and 11.6 mmol/(m^2 day).

Glüd (2008) reviews the status of oxygen dynamics in a heavily referenced paper that summarizes total oxygen uptake (TOU) data from over 54 *in situ* studies in a plot of TOU versus water depth. Values of TOU range from over 50 mmol/m^2 day at 10 m depth at nearshore sites to less than 1 mmol/m^2 day at several thousand meters depth. Our 160-day mean maximum value of 11.6 mmol/m^{2}day is near the top but within the range of values observed near 882 m depth. Our relatively high TOU values can be attributed to the high benthic activity that characterizes the MC118 Woolsey Mound in general. The NW crater area, in particular, features active hydrocarbon seeps and contains high concentrations of bacterial mats (Lloyd et al., 2010), oil and gas (Lapham et al., 2008b), and high rates of biogenic methane production (Lapham et al., 2008b).

Four-week averaged values of ambient and chimney DO concentrations reveal up to 29% and 51% declines in chimney DO concentrations measured independently at 28.4 and 20.3 cm respectively above the seafloor relative to ambient BBL DO concentrations. Low DO concentrations in the chimneys occur throughout the record, however, the four-week averaged values indicate a distinct minimum from January through February 2012, at both heights above the seafloor (Fig. 8, middle panel, red dashed line). Higher currents and increased chimney washout in December (Fig. 5) may have obscured decreased DO values resulting from TOU during that month, however, this temporal variability is not strictly related to current speed as little drawdown is observed in April when currents are generally low.

5. Conclusions

1. Current velocities during the 160-day deployment ranged from near zero to over 22 cm/s in bursts sustained for multiple days (Fig. 5). The mean (vector-averaged) current over the deployment period was 2.6 cm/s toward 305°. The dominantly SE to NW flow, including nearly all flow greater than 15 cm/s, was parallel to the local topography (see Fig. 1 above) and strongest towards 320°. Observations of warmer water during upslope (NW) flow indicated that complex bottom topography can greatly influence local water transport in the BBL on the northern Gulf upper slope.
2. Ambient DO concentrations within the BBL are controlled by cross-slope movement of water masses. DO concentrations exhibit a nearly linear inverse correlation with temperature and depend on the change in proportions of AAIW versus TACW water masses. When tested against other deep water data sets from the northern Gulf this correlation should allow for accurate calculations of DO deficits resulting from localized processes including consumption associated with gas and oil releases.
3. A combination of continuous current speed and conventional oxygen optode measurements of concentration gradients within an open cylinder flux chamber (chimney) on the seafloor appear sufficient to quantify maximum values of TOU for sustained periods in the deep sea. The relatively simple CSA system has produced a 160-day, continuous data set with an average sediment TOU of 11.6 mmol/m^2 day. This time-series, *in situ* data improves our understanding of temporal variability in TOU by upper slope sediments using methodology available to many deep-sea researchers.
4. Chimney DO concentrations measured during the 21-day deployment exhibited quasi-daily variations that were not observed during the longer 160-day deployment at a site featuring different topography. We hypothesize that these near-daily variations were the result of an interaction between

near inertial waves and the steep topography of the "horseshoe" scarp immediately adjacent to the 21-day deployment site that modulated currents at the top of the chimney.

5. Dissolved methane concentrations in the BBL at our MC118 site are elevated relative to atmospheric equilibration values expected for *in situ* temperatures and salinities. These higher methane concentrations most likely result from sediment gas bubble release from natural gas seeps, partial bubble dissolution and horizontal, advective transport of gas-rich plumes within meters of the seafloor. Longer term methane time-series data combined with current velocity and direction data should allow monitoring of sites of gas release, whether natural or accidental.

Our 160-day lander deployment at MC118 has provided a robust data set that reveals new capabilities for long-term monitoring of near-bottom processes in biogeochemically active, continental margin environments using free lander vehicles. Long term *in situ* monitoring combined with an understanding of dominant physical and biogeochemical processes can contribute significantly to quantifying the fate and impacts of gas and oil releases over time scales of months to years.

Acknowledgments

We remember Robert Woolsey, Director of the Mississippi Minerals Research Institute (MMRI) at the University of Mississippi (UM), for his support of our efforts to begin sustained physical and chemical monitoring efforts at lease block MC118. Matt Lowe, MMRI, led the design and construction of the ROVARD lander. He also directed deployment and recovery operations, assisted by MMRI team members including Andy Gossett, Brian Noakes, and Larry Overstreet. Dan Hoer, UNC-Chapel Hill, assisted with CSA system preparation and the 2010 ROVARD deployment. Final at-sea deployment site choices were made by Ken Sleeper based on his extensive knowledge of previous research at block MC118; Carol Lutken provided additional information about the geological characteristics of the sites. We thank the captain and crew members of the R/V *Pelican* for their excellent assistance with deployment and retrieval activities during multiple cruises, Chuck Fisher, PSU, Chief Scientist during BOEM/NOAA *Lophelia* II project for ROV Jason II observations of the ROVARD lander during the 2010 deployment. Eric Cordes, Chief Scientist of the E/V *Nautilus* NRDA cruise with ROV *Hercules* for photo of the ROVARD on the seafloor. We thank members of the ECOGIG Project research team for their comments and contributions to the completed research. We thank two anonymous reviewers of the original manuscript for insightful criticisms and suggestions. This research was made possible in part by a grant from The Gulf of Mexico Research Initiative (GoMRI) to support the ECOGIG consortium, and in part by the Gulf of Mexico Hydrate Research Consortium sub-contract grant no. 300212260E from the University of Mississippi to UNC-Chapel Hill (CSM). Data are publicly available through the Gulf of Mexico Research Initiative Information & Data Cooperative (GRIIDC) at https://data.gulfresearchinitiative.org (UDI's: < R1.x132.134:0122 > and < R1.x132.134:0124 > . This is ECOGIG contribution #374.

References

Carnes, M.R., Teague, W.J., Jarosz, E., 2008. Low-frequency current variability observed at the shelfbreak in the northeastern Gulf of Mexico: November 2004–May 2005. Cont. Shelf Res. 28, 399–423.

Chanton, J.P., Cherrier, J., Wilson, R.M., Sarkodee-Adoo, J., Bosman, S., Mickle, A., Graham, W.M., 2012. Radiocarbon evidence that carbon from the Deepwater Horizon spill entered the planktonic food web of the Gulf of Mexico. Environ. Res. Lett. 7, 1–4.

Dade, W.B., Hogg, A.J., Boudreau, B.P., 2001. 2 Physics of flow above the sediment–water interface. In: Boudreau, B.P., Jørgensen, B.B. (Eds.), The Benthic Boundary Layer, pp. 4–43.

Davies, A.J., Duineveld, G.C.A., Weering, T.C.Ev, Mienis, F., Quattrini, A.M., Seim, H.E., Bane, J.M., Ross, S.W., 2010. Short-term environmental variability in cold-water coral habitat at Viosca Knoll, Gulf of Mexico. Deep-Sea Res. I 57, 199–212.

Glüd, R.N., Gundersen, J.K., Revsbech, N.P., Jøorgensen, B.B., Hüttel, M., 1995. Calibration and performance of the stirred flux chamber from the benthic lander Elinor. Deep-Sea Res. I 42, 1027–1042.

Glüd, R.N., Berg, P., Fossing, H., Jørgensen, B.B., 2007. Effect of the diffusive boundary layer on benthic mineralization and O_2 distribution: A theoretical model analysis. Limnol. Ocean. 52, 547–557.

Glüd, R.N., 2008. Oxygen dynamics of marine sediments. Mar. Biol. Res. 4, 243–289.

Hallock, Z.R., Teague, W.J., Jarosz, E., 2009. Subinertial slope-trapped waves in the northeastern Gulf of Mexico. J. Phys. Ocean. 39, 1475–1485.

Holtappels, M., Kuypers, M.M.M., Schlüter, Brüchert, V., 2011. Measurement and interpretation of solute concentration gradients in the benthic boundary layer. Limnol. Ocean.: Methods 9, 1–13.

Ingram, W.C., Meyers, S.R., Martens, C.S., 2013. Chemostratigraphy of deep-sea Quaternary sediments along the Northern Gulf of Mexico Slope: quantifying the source and burial of sediments and organic carbon at Mississippi Canyon 118. Mar. Pet. Geol. 46, 190–200.

Jochens, A.E., DiMarco, S.F., 2008. Physical oceanographic conditions in the deepwater Gulf of Mexico in summer 2000–2002. Deep-Sea Res. II 55, 2541–2554.

Joye, S.B., MacDonald, I.R., Leifer, I., Asper, V., 2011. Magnitude and oxidation potential of hydrocarbon gases released from the BP oil well blowout. Nat. Geosci. 4, 160–164.

Joye, S.B., Teske, A., Kostka, J.E., 2014. Microbial dynamics following the Macondo Oil Well Blowout across Gulf of Mexico environments. Bioscience 64 (9), 766–777.

King, C., Martens, C.S., Cordes, E., 2015. Oxygenation concentrations in deep-water coral communities of the northern Gulf of Mexico. GoMRI Annual Meeting Abstracts, Houston, TX, January 2015.

Lapham, L., Wilson, R., Riedel, M., Paull, C.K., Holmes, M.E., 2013. Temporal variability of in situ methane concentrations in gas hydrate-bearing sediments near Bullseye Vent. Geochem. Geophys. Geosyst. 14 (7), 2445–2459.

Lapham, L.L., Chanton, J.P., Martens, C.S., Higley, P.D., Jannasch, H.W., Woolsey, J.R., 2008a. Measuring temporal variability in pore-fluid chemistry to assess gas hydrate stability: development of a continuous pore-fluid array. Environ. Sci. Technol. 42 (19), 7368–7373.

Lapham, L.L., Chanton, J.P., Martens, C.S., Sleeper, K., Woolsey, J.R., 2008b. Microbial activity in surficial sediments overlying acoustic wipe-out zones at a Gulf of Mexico cold seep. Geochem. Geophys. Geosyst. 9 (6), Q06001, doi: 06010.01029/02008GC001944.

Lapham, L.L., Wilson, R.M., MacDonald, I.R., Chanton, J.P., 2014. Gas hydrate dissolution rates quantified with laboratory and seafloor experiments. Geochim. Et. Cosmochim. Acta 125, 492–503.

Lloyd, K.G., Albert, D.B., Biddle, J.F., Chanton, J., Pizarro, O., Teske, A., 2010. Spatial structure and activity of sedimentary microbial communities underlying a Beggiatoa spp. mat in a Gulf of Mexico hydrocarbon seep. Plos One 5 (1), e8735.

MacDonald, I.R., Buthman, D.B., Sagar, W.W., Peccini, M.B., Guinasso Jr, N.L., 2000. Pulsed oil discharge from a mud volcano. Geology 28 (10), 907–910.

MacDonald, I.R., Guinasso Jr., N.L., Sassen, R., Brooks, J.M., Lee, L., Scott, K.T., 1994. Gas hydrate that breaches the sea floor on the continental slope of the Gulf of Mexico. Geology 22, 699–702.

Macelloni, L., Brunner, C.A., Caruso, S., Lutken, C.B., D'Emidio, M., Lapham, L.L., 2013. Spatial distribution of seafloor bio-geological and geochemical processes as proxies of fluid flux regime and evolution of a carbonate/hydrates mound, northern Gulf of Mexico. Deep. Sea Res. I 74, 25–38.

Macelloni, L., Simonetti, A., Knapp, J.H., Knapp, C.C., Lutken, C.B., Lapham, L.L., 2012. Multiple resolution seismic imaging of a shallow hydrocarbon plumbing system, Woolsey Mound, Northern Gulf of Mexico. Mar. Pet. Geol. 38, 128–142.

Mau, S., Rehder, G., Arroyo, I.G., Gossler, J., 2007. Indications of a link between seismotectonics and CH4 release from seeps off Costa Rica. Geochem. Geophys. Geosyst. 8 (4). http://dx.doi.org/10.1029/2006GC001236.

McGee, T., 2006. A seafloor observatory to monitor gas hydrates in the Gulf of Mexico. Seg. Lead. Edge, 644–647.

McGinnis, D.F., Sommer, S., Lorke, A., Glüd, R.N., Linke, P., 2014. J. Geophys. Res. Ocean. 119, 6918–6932.

Mienis, F., Duineveld, G.C.A., Davies, A.J., Ross, S.W., Seim, H., Bane, J., Weering, T.C. E., 2012. he influence of near-bed hydrodynamic conditions on cold-water corals in the Viosca Knoll area, Gulf of Mexico. Deep-Sea Res. I 60, 32–45.

Morrison, J.M., Merrell Jr., W.J., Key, R.M., Key, T.C., 1983. Property distributions and deep chemical measurements within the western Gulf of Mexico. J. Geophys. Res. Lett. 88 (C4), 2601–2608.

Passow, U., 2016. Formation of rapidly-sinking, oil-associated marine snow. Deep. Sea Res. II 129, 232–240.

Rivas, D., Badan, A., Ochoa, J., 2005. The ventilation of the deep Gulf of Mexico. J. Phys. Ocean. 35, 1763–1781.

Roberts, J.M., Wheeler, A., Freiwald, A., Cairns, S., 2009. Cold-Water Corals. Cambridge University Press.

Røy, H., Hüttel, M., Jørgensen, B.B., 2005. The influence of topography on the functional exchange surface of marine soft sediments, assessed from sediment topography measured in situ. Limnol. Ocean. 50, 106–112.

Sassen, R., Roberts, H.H., Jung, W., Lutken, C.B., DeFreitas, D.A., Sweet, S.T., Guinasso Jr., N.L., 2006. The Mississippi Canyon 118 Gas Hydrate Site: a complex natural system. OTC Paper #18132; Offshore Technology Conference, Houston, TX.

Seim, H.E., Kjerfve, B., Sneed, J.E., 1987. Tides of Mississippi Sound and the adjacent continental shelf. Estuaries Coast. Shelf Sci. 25, 143–156.

Simonetti, A., Knapp, J.H., Sleeper, K., Lutken, C.B., Macelloni, L., Knapp, C.C., 2013. Spatial distribution of gas hydrates from a high-resolution seismic and core data, Woolsey Mound, Gulf of Mexico. Mar. Pet. Geol. 44, 21–33.

Sleeper, K., Rachel Wilson, Jeffery Chanton, Laura Lapham, Norman Farr, Richard Camilli, Christopher Martens, Pontbriand, C., 2011. Geochemical Arrays at Woolsey Mound Seafloor Observatory (Abstract OS13C-1545). American Geophysical Union Fall Meeting, San Francisco, CA.

Sturges, W., Lugo-Fernandez, A., 2005. Circulation in the Gulf of Mexico: Observations and Models, Geophysical Monograph Series, vol. 161. American Geophysical Union.

Thomsen, L., Barnes, C., Best, M., Chapman, R., Pirenne, B., Thomson, R., Vogt, J., 2012. Ocean circulation promotes methane release from gas hydrate outcrops at the NEPTUNE Canada Barkley Canyon node. Geophys. Res. Lett. 39 (L16605).

Torres, M.E., Trehu, A., Riedel, M., Paull, C., Davis, E., 2007. Gas-Hydrate Observatories Workshop (GHOBS) Report. Portland.

Trowbridge, J.H., Geyer, W.R., Bowen, M.M., Williams III, A.J., 1999. Near-bottom turbulence measurements in a partially mixed estuary: turbulent energy balance, velocity structure, and along-channel momentum balance. J. Phys. Ocean. 29, 3056–3072.

White, H.K., Hsing, P.-Y., Cho, W., Shank, T.M., Cordes, E.E., Quattrini, A.M., Nelson, R. K., Camilli, R., Demopoulos, A.W.J., German, C.R., Brooks, J.M., Roberts, H.H., Shedd, W., Reddy, C.M., Fisher, C.R., 2012. Impact of the Deepwater Horizon oil spill on a deep-water coral community in the Gulf of Mexico. Proc. Natl. Acad. Sci. 109 (50) 20303–20308.

Wilson, R.M., Macelloni, L., Simonetti, A., Lapham, L., Lutken, C., Sleeper, K., D'Emidio, M., Pizzi, M., Knapp, J., Chanton, J., 2014. Subsurface methane sources and migration pathways within a gas hydrate mound system, Gulf of Mexico. Geochem. Geophys. Geosyst. 15 (1), 1–19.